Journal of Gastrointestinal Cancer (2019) 50:91–97
https://doi.org/10.1007/s12029-017-0035-6

ORIGINAL RESEARCH

Differential Diagnosis of Pancreatic Epidermoid Cyst Without a Solid Component (Residual Splenic Tissue) vs. Mucinous Cystic Neoplasm

Kousei Ishigami[1] · Akihiro Nishie[1] · Hiroyuki Irie[2] · Yoshiki Asayama[1] · Yasuhiro Ushijima[1] · Yukihisa Takayama[1] · Daisule Okamoto[1] · Nobuhiro Fujita[1] · Takao Ohtsuka[3] · Tetsuhide Ito[4] · Naoki Mochidome[5] · Hiroshi Honda[1]

Published online: 7 December 2017

Abstract

Purpose The purpose of this study was to clarify whether there are differences in imaging findings between pancreatic epidermoid cyst (EDC) without a solid component (residual splenic tissue) and mucinous cystic neoplasm (MCN).

Materials and Methods The study group consisted of histologically proven EDC (eight cases) and MCN (20 cases). CT and MRI findings were compared on the following imaging findings: the shape of the cystic lesions and the presence or absence of septum, calcification, and high-intensity fluid on T1- and diffusion-weighted images (*b* factor = 1000). The degree of contact with the pancreatic tail was compared between the EDCs and six of the MCNs at the edge of the pancreatic tail.

Results The EDCs were round ($n = 3$) or oval ($n = 5$), while the MCNs consisted of three round, five oval, six pear-like, and six multilobulated lesions ($P < 0.05$). Septum was present in 4 of 8 (50%) EDCs and 19 of 20 (95%) MCNs ($P < 0.05$). The presence of calcification (2 of 8 [25%] EDCs vs. 8 of 20 [40%] MCNs), high-intensity fluid on T1-weighted images (2 of 7 [29%] EDCs vs. 5 of 20 [25%] MCNs), and high-intensity fluid on diffusion-weighted images (5 of 7 [71%] EDCs vs. 5 of 20 [25%] MCNs) were not significantly different. The degree of contact with the pancreatic parenchyma was similar between the two types of lesions.

Conclusion Although the imaging findings for EDC without a solid component and MCN overlap, a pear-like or multilobulated shape may favor a diagnosis of MCN.

Keywords Pancreas · Epidermoid cyst · Mucinous cystic neoplasm · CT · MRI

Introduction

Pancreatic epidermoid cyst (EDC) is a rare non-neoplastic true cyst of the pancreas. Because the pancreatic EDC originates from an intrapancreatic accessory spleen, EDC presents as a cystic lesion at the edge of the pancreatic tail [1].

The radiological diagnosis of pancreatic EDC may be rendered if residual splenic tissue can be recognized, showing imaging characteristics similar to the normal spleen (i.e., similar attenuation, signal intensity, or enhancement pattern) [2–5]. In addition, superparamagnetic iron oxide (SPIO)-enhanced MRI can confirm the presence of residual splenic tissue [6].

Through our clinical experiences, however, it is not always possible to suggest the presence of residual splenic tissue on imaging findings, especially when EDC presents as a completely cystic mass without a solid component. If residual splenic tissue cannot be recognized, radiological differential diagnosis of EDC vs. mucinous cystic neoplasm (MCN) is challenging [7, 8]. In addition, both EDC and MCN may present with an elevated serum carbohydrate antigen 19-9 (CA19-9) level [9–11]. Cyst fluid analysis from endoscopic

✉ Kousei Ishigami
ishigami@radiol.med.kyushu-u.ac.jp

[1] Department Clinical Radiology, Graduate School of Medical Sciences, Kyushu University, 3-1-1 Maidashi, Higashi-ku, Fukuoka City 812-8582, Japan

[2] Department of Radiology, Faculty of Medicine and Graduate School of Medicine, Saga University, Saga, Japan

[3] Department Surgery and Oncology, Graduate School of Medical Sciences, Kyushu University, Fukuoka City, Japan

[4] Department Medicine and Bioregulatory Science, Graduate School of Medical Sciences, Kyushu University, Fukuoka City, Japan

[5] Anatomic Pathology, Graduate School of Medical Sciences, Kyushu University, Fukuoka City, Japan

Table 1 MDCT protocols

MDCT	IV contrast material	Volume	injection rate	PPP	PV	EP	Section thickness
4-Channel (3-phase)	350 or 370 mgI/mL[a]	100 mL	2.5 mL/s	45 s	70 s	240 s	3 mm
4-Channel (2-phase)	300 mgI/mL[b]	100 mL	2.5 mL/s	NA	70 s	240 s	5 mm
4-Channel (unenhanced)	NA	NA	NA	NA	NA	NA	5 mm
64-Channel (3-phase)	350 or 370 mgI/mL	NA	3.3 mL/s	35 s	60 s	60 s	1 and 3 mm

MDCT multidetector-row computed tomography, *IV* intravenous, *PPP* pancreatic parenchymal phase, *PV* portal venous phase, *EP* equilibrium phase, *NA* not applicable

[a] Three hundred seventy milligrams or 350 mg I/mL IV contrast material: iopamidol, Iopamiron 370, Bayer Schering Pharma, Japan; or iohexol, Omnipaque 350, Daiichi Sankyo, Japan

[b] Three hundred milligrams of iodine per milliliter of IV contrast material: iopamidol, Iopamiron 300, Bayer Schering Pharma, Japan

ultrasound (EUS) may show high CA19-9 and CEA, which may cause erroneous diagnosis of mucinous neoplasms, and EUS-guided fine needle aspiration for EDC may be occasionally non-specific, revealing macrophages and scattered small lymphocytes [12]. It is important to distinguish MCN from EDC for clinical management, because surgical resection should be considered for MCN [13].

The purpose of this study was to clarify whether there are differences in imaging findings between pancreatic EDC without a solid component (radiologically apparent residual splenic tissue) and MCN.

Materials and Methods

Patient Population

Between August 2000 and September 2010, a computerized search of the institutional radiology database, clinical records, and pathology reports found 8 cases of pancreatic epidermoid cyst (EDC) from 2 institutions, and 20 cases of mucinous cystic neoplasm (MCN) from 1 institution, all of whom had undergone surgical resection and preoperative imaging studies including CT ($n = 28$) and MRI ($n = 27$).

In the pancreatic EDC group ($n = 8$), all eight patients were female. The ages ranged from 26 to 70 years (mean ± standard deviation [SD] 46 ± 16 years old). The size of the lesions ranged from 2.0 to 6.6 cm (mean ± SD 4.1 ± 1.7 cm). All lesions were noted at the edge of the pancreatic tail. A solid component was not recognized in any of these eight cases based on either imaging or macroscopic findings.

In the pancreatic MCN group ($n = 20$), there were 19 female patients and 1 male patient. The ages ranged from 17 to 76 years (mean ± SD 43 ± 15 years old). The size of the lesions ranged from 2.5 to 9.1 cm (mean ± SD 5.2 ± 1.8 cm). MCN was noted in the pancreatic body ($n = 9$) or tail ($n = 11$). In addition, six cases were seen at the edge of the pancreatic tail.

Table 2 MRI protocols

Unenhanced images	T2WI	T1WI	MRCP	DWI	
	Axial SSTSE with FS	Axial GRE with FS	Axial and coronal 2D-MRCP	Single-shot EPI	
	Axial TSE with FS	Axial dual echo GRE	Coronal 3D-MRCP	MPG pulses: 3 axes	
			MIP images (2D and 3D)	*b* factor = 0, 500, 1000 s/mm^2	
CE study	Arterial phase	Portal phase	Late portal phase	Equilibrium phase	Post-contrast
	Test injection method	Arterial phase + 30 s	90 s	240 s	Axial or coronal

T2WI T2-weighted image, *T1WI* T1-weighted image, *MRCP* magnetic resonance (MR) cholangiopancreatography, *DWI* diffusion-weighted image, *SSTSE* single-shot turbo spin echo, *FS* fat saturation, *GRE* gradient echo, *D* dimensional, *MIP* maximum intensity projection, *EPI* echo planar image, *MPG* motion-probing gradient, *CE* contrast-enhanced

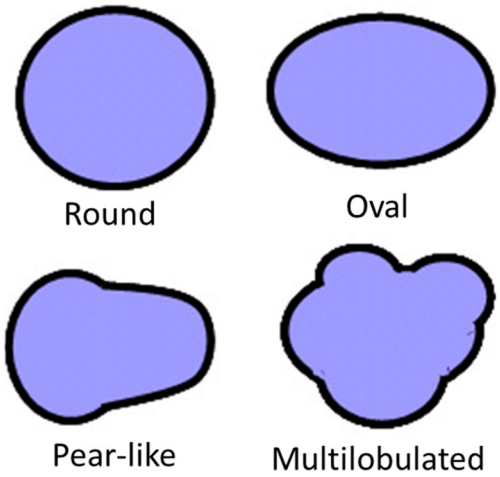

Fig. 1 Schematic drawing of the shape of the cystic lesions

There were no significant differences in the mean age of the patients ($P = 0.680$) or the mean size of the lesions ($P = 0.162$) between pancreatic EDC and MCN.

Imaging Technique

CT and MRI scan units and protocols were various because the patients were recruited over a long period of time (10 years). CT and MRI protocols are summarized in Tables 1 and 2.

CT studies were performed in all of the 28 patients using a 4-channel (Aquilion, Toshiba, Japan [$n = 10$], or Volume Zoom, Siemens, Germany [$n = 3$]) or 64-channel (Aquilion, Toshiba, Japan [$n = 15$]) multidetector-row CT (MDCT). MRI studies were performed in 27 cases using a 1.5-T (Intera Achieva, Philips, Netherlands [$n = 12$], MAGNETOM Symphony [$n = 6$], Vision [$n = 4$], Avanto [$n = 1$], Siemens, Germany) or a 3-T (Intera Achieva, Philips, Netherlands [$n = 4$]) MR unit.

All patients with pancreatic EDC ($n = 8$) underwent three-phase contrast-enhanced (CE) dynamic MDCT. MRI including diffusion-weighted images was also performed in seven cases. CE-MRI was performed in six cases, and CE-dynamic MRI was available in four cases.

Among the patients with pancreatic MCN ($n = 20$), 19 underwent CE two-phase ($n = 1$) or three-phase ($n = 18$) MDCT, and the remaining patient underwent unenhanced CT. MRI including diffusion-weighted images was performed in all 20 patients. CE-MRI was performed in 19 cases, and CE-dynamic MRI was available in 9 cases.

For Siemens MR scanners ($n = 11$), diffusion-weighted images (DWI) were obtained while the patients held their breath, and a fat-saturated pulse was used to exclude severe chemical shift artifacts. For Philips MR scanners ($n = 16$), DWI were obtained by the respiratory gating technique, and spectral presaturation inversion recovery was utilized.

CE (gadopentetate dimeglumine: Magnevist Syringe, Bayer Schering Pharma, Japan) three-dimensional dynamic MRI studies were performed in 13 cases at an injection rate of 2.0 cm^3/s. In addition, post-contrast axial or coronal T1-weighted gradient echo (GRE) images (T1WI) with fat saturation were available in 25 cases.

Table 3 The shape of pancreatic epidermoid cyst (EDC) and mucinous cystic neoplasm (MCN)

	Round	Oval	Pear-like	Multilobulated
EDC	3	5	0	0
MCN	3	5	6	6

EDC showed a round or oval shape, and a pear-like or multilobulated shape was seen only in MCN ($P < 0.05$, Kruskal-Wallis test)

Imaging Analysis

Two experienced abdominal imaging radiologists who were blinded to the final diagnosis randomly reviewed 28 MDCT and 27 MRI studies in a consensus fashion.

The signal intensity of the cyst wall was subjectively assessed on T2-weighted images (T2WI). One of the reviewers measured the thickness of the cyst wall in the equilibrium phase of CE-CT. The reviewer selected two portions where the cyst wall appeared thickest and thinnest, and magnified the image on a computer workstation. When measuring the thinnest portion, the reviewer avoided the portion where wall enhancement was invisible. Each measurement was performed twice, and the average data were recorded. For this measurement, one EDC that was not stored in the computer workstation and one MCN that had undergone unenhanced CT were excluded.

The shape of the cystic lesions was classified into the following four types: round, oval, pear-like, and multilobulated (Fig. 1). When evaluating the shape, the reviewer utilized not only axial images but also coronal MR cholangiopancreatography (MRCP), coronal post-contrast T1WI when available, and MPR images from MDCT. In two MCN cases, MDCT studies were performed with a 5-mm section thickness. MPR images from MDCT were not utilized for these two cases, but coronal MRCP was available for review.

The presence or absence of calcification was assessed based on CT. The presence or absence of septum was assessed based on CE-MDCT/MRI and axial/coronal MRCP.

The signal intensity of cyst fluid was assessed by T1WI and high b factor ($b = 1000$) DWI. When cyst fluid showed high intensity, the reviewers recorded the data. The apparent diffusion coefficient (ADC) was not compared because MRI units were various.

The degree of contact with the pancreatic parenchyma was compared between all EDC cases ($n = 8$) and six of the MCN cases at the edge of the pancreatic tail. For this evaluation, the

Table 4 Comparison between pancreatic epidermoid cyst (EDC) and mucinous cystic neoplasm (MCN)

	EDC	MCN	*P* value
Septum	4 (50%)	19 (95%)	< 0.05[a]
Multiple septa (shape)	1 (oval)	8 (oval 1, pear-like 1, multilobulated 6[b])	
One or a few septa (shape)	3 (round 1, oval 2)	11 (round 2, oval 4, pear-like 5)	
Calcification	2 (25%)	8 (40%)	n.s.
High-intensity fluid on T1WI	2 (29%)	3 (15%)	n.s.
High-intensity fluid on DWI	5 (71%)	5 (25%)	n.s.

[a] There was a significant difference in the presence or absence of septum between pancreatic EDC and MCN

[b] Septum is seen in 95% of MCNs, and six of eight MCNs with multiple septa showed a lobulated shape. There were no significant differences in the presence or absence of calcification, high-intensity fluid on T1-weighted images (T1WI), or high-intensity fluid on high *b* value ($b = 1000$) diffusion-weighted images (DWI)

degree of contact with the pancreatic parenchyma was categorized as follows: less than one third of the cyst margin, more than one third but less than half of the cyst margin, and more than half of the cyst margin. In addition, if the cystic lesion abutted on the spleen, the reviewers recorded the data.

Statistical Analysis

The thickness of the cyst wall of the pancreatic EDC and MCN was compared by Student's or Welch's *t* test. The shape of the cystic lesions was compared using the Kruskal-Wallis

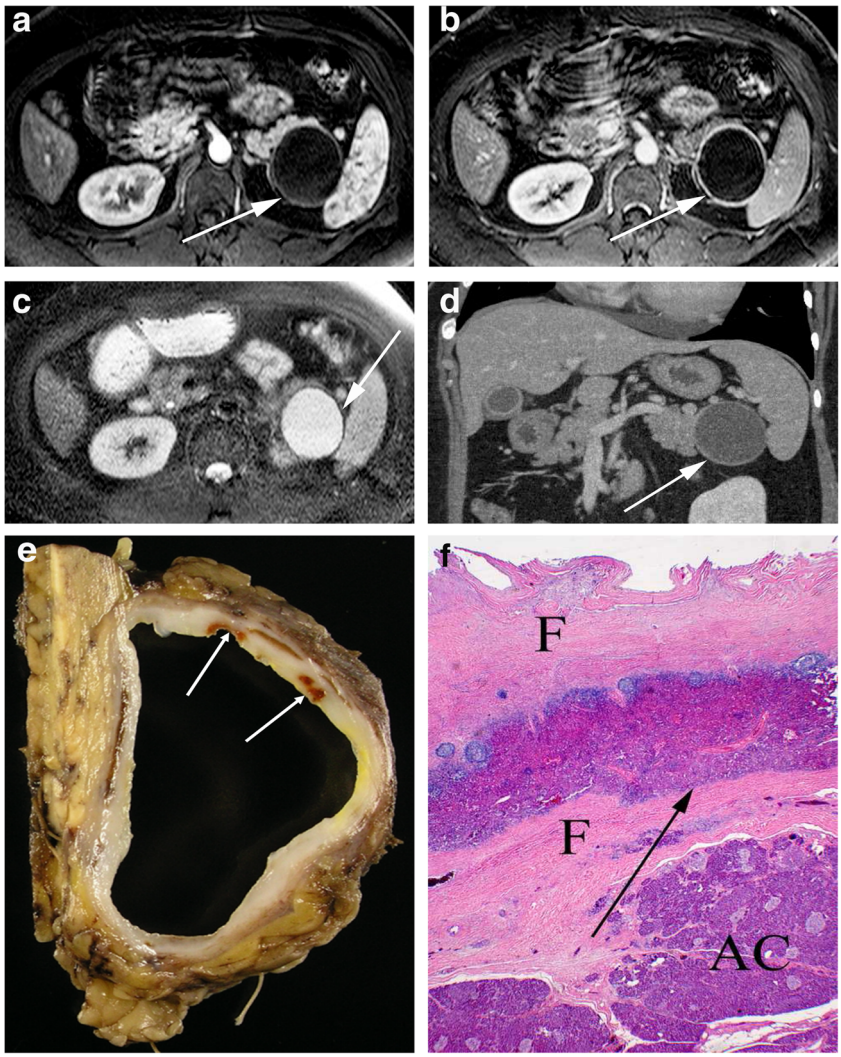

Fig. 2 A 35-year-old female with pancreatic epidermoid cyst (EDC). **a** The arterial phase of the axial contrast-enhanced (CE) dynamic T1-weighted gradient echo (GRE) with fat saturation (FS) image shows a well-circumscribed unilocular cystic mass at the edge of the pancreatic tail (arrow). **b** The equilibrium phase of the axial CE dynamic T1-weighted GRE with FS image shows the delayed enhancement of the cyst wall (arrow). **c** Axial T2-weighted single-shot turbo spin-echo (TSE) with FS image shows low intensity of the cyst wall (arrow). **d** Coronal oblique reformatted image obtained from the portal venous phase shows a well-circumscribed round-shaped cystic mass at the edge of the pancreatic tail (arrow). **e** Macroscopic view. The resected specimen after formalin fixation shows a small amount of splenic tissue within the cyst wall (arrow). **f** A microscopic view (hematoxylin-eosin stain × 12.5) from the resected specimen shows that the cyst wall consists of abundant fibrosis (F) and residual splenic tissue (arrow). AC indicates pancreatic acinar tissue of the pancreatic parenchyma

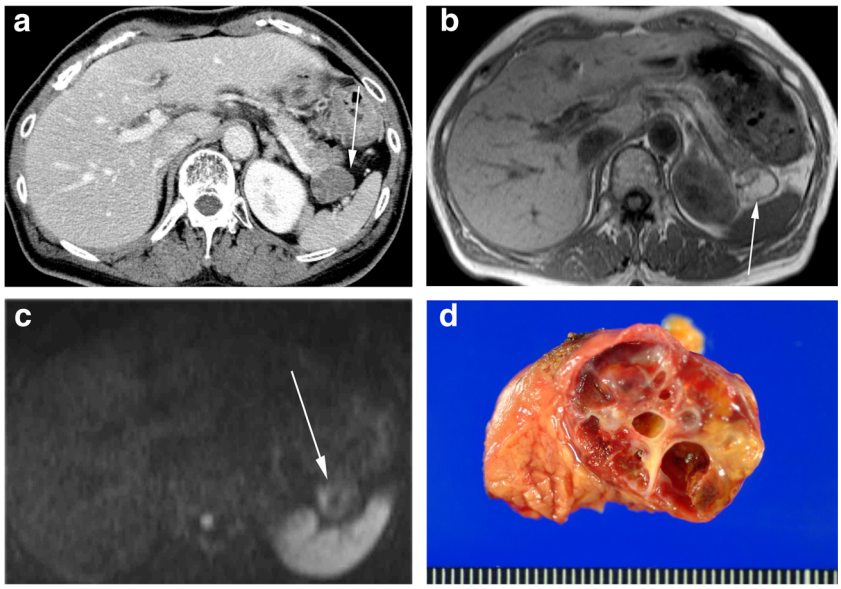

Fig. 3 A 70-year-old female with EDC with multiple septa. **a** The portal venous phase of axial CT shows an oval-shaped cystic mass with multiple septa (arrow). **b** Axial T1-weighted GRE image shows the high-intensity fluid in the cystic lesion (arrow). **c** Axial diffusion-weighted image (*b* factor = 1000) shows the high intensity of the lesion (arrow). **d** Macroscopic view of the resected specimen shows multiple septa within the cystic lesion. No solid component suggestive of splenic tissue is seen

test. The presence or absence of high-intensity fluid, calcification, and septum was compared by Fisher's exact test. A *P* value of less than 0.05 was considered statistically significant.

Results

The results are summarized in Tables 3 and 4.

In our series, there was no solid component in either pancreatic epidermoid cyst (EDC) or mucinous cystic neoplasm (MCN). The cyst wall showed low intensity relative to the normal spleen on T2WI (Fig. 2), and a high-intensity component within the cyst wall was not observed on diffusion-weighted images in either EDC or MCN cases. In addition, contrast enhancement of the cyst wall could be most clearly appreciated in the equilibrium phase of contrast-enhanced CT/MRI (Fig. 2). The thickest measured portion of the cyst wall of EDC ranged from 1.8 to 3.8 mm (mean ± standard deviation [SD] 2.4 ± 0.7 mm), and that of MCN ranged from 1.3 to 3.8 (mean ± SD 2.3 ± 0.7 mm) ($P = 0.812$). In contrast, the thinnest measured portion of the cyst wall of EDC ranging from 1.3 to 2.3 mm (mean ± SD 1.6 ± 0.4 mm), and that of MCN ranged from 0.8 to 1.5 (mean ± SD 1.1 ± 0.2 mm) ($P = 0.008$, Welch's *t* test).

In the patients with EDC ($n = 8$), the lesions were round ($n = 3$) (Fig. 1) or oval ($n = 5$) (Fig. 3). Among the 20 cases of pancreatic MCN, 3 lesions were round, 5 oval, 6 pear-like (Fig. 4), and 6 multilobulated (Fig. 5). There was a significant difference in the shape of the cystic lesions between the EDCs and MCNs ($P = 0.00281$). Septum was seen in 4 of 8 (50%) EDCs, while it was seen in 19 of 20 (95%) MCNs ($P = 0.0148$). Three of four EDCs showed one or only a few septa peripherally, and the remaining EDC had multiple septa (Fig. 3). In addition, all of the six MCNs with a lobulated shape had multiple septa (Fig. 5).

If the diagnostic criterion of MCN was set as pear-like/multilobulated shape and the presence of septum, the sensitivity, specificity, positive predictive value, and negative predictive value were 60, 100, 100, and 50%, respectively. If it was set as either pear-like/multilobulated shape or the presence of septum, the sensitivity, specificity, positive predictive value, and negative predictive value were 95, 50, 82.6, and 80%, respectively.

There were no significant differences in the presence of calcification (2 of 8 [25%] EDCs vs. 8 of 20 [40%] MCNs,

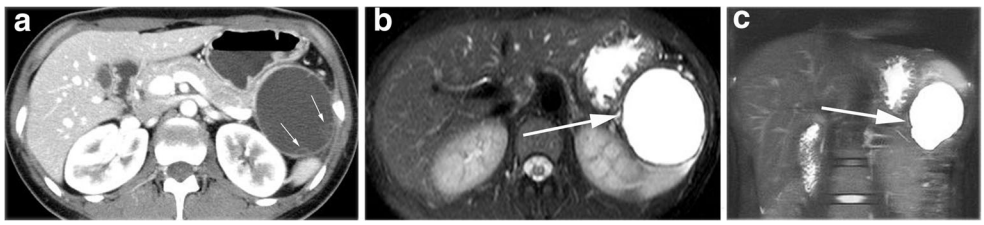

Fig. 4 A 23-year-old female with mucinous cystic neoplasm (MCN) showing a pear-like shape. **a** The portal venous phase of axial CT shows a well-circumscribed cystic mass with wall enhancement at the tail of the pancreas. There are a few septa (arrows) peripherally. **b** Axial T2-weighted TSE with FS image shows the low intensity of the cyst wall (arrow). The findings of axial images (**a**, **b**) mimic EDC (see Fig. 2a–c). **c** Coronal T2-weighted MR cholangiopancreatography (MRCP) demonstrates the pear-like shape of the cystic lesion (arrow)

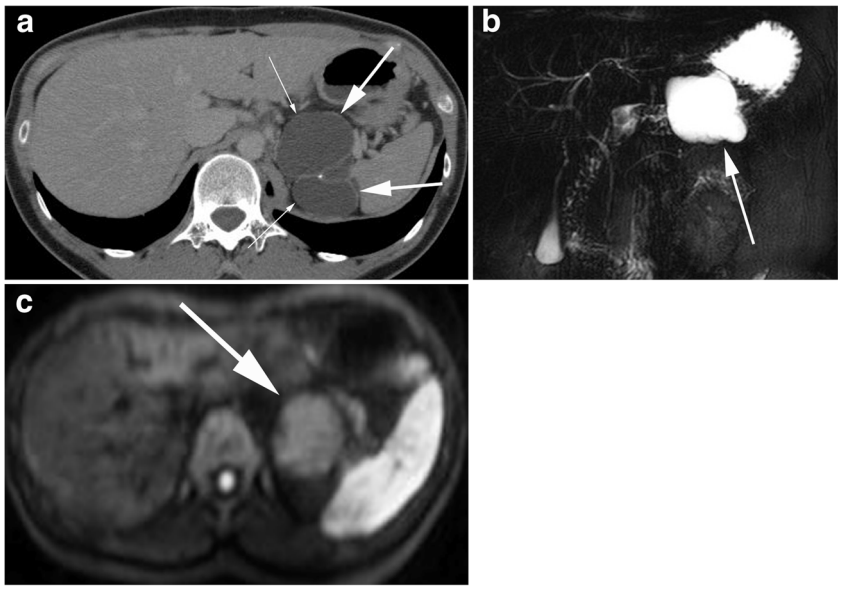

Fig. 5 A 39-year-old female with MCN showing a multilobulated shape. **a** The equilibrium phase of axial CE-CT shows a multilocular cystic mass at the edge of the pancreatic tail. Wall enhancement is visible (large arrows). However, the cyst wall is invisible in some portions (small arrows). **b** A maximum intensity projection (MIP) image of MRCP clearly shows the lobulated contour of the cystic lesion (arrow). **c** An axial diffusion-weighted image (*b* factor = 1000) shows the high intensity of the lesion (arrow). In this case, fluid-fluid levels owing to hemorrhage were seen on T1-weighted and T2-weighted images (not shown)

$P = 0.669$), high-intensity fluid on T1WI (2 of 7 [29%] EDCs vs. 3 of 20 [15%] MCNs, $P = 0.580$), or high-intensity fluid on diffusion-weighted images (5 of 7 [71%] EDCs vs. 5 of 20 [25%] MCNs, $P = 0.0647$).

The degree of contact with the pancreatic parenchyma was similar between EDC and MCN at the edge of the pancreatic tail ($n = 6$). In EDCs, five of eight lesions abutted on the pancreatic parenchyma by less than one third of the cyst margin, and three did so by less than half. In MCNs, four of six lesions abutted on the pancreatic parenchyma by less than one third of the cyst margin, and two did so by less than half. In addition, seven of eight (87.5%) EDCs abutted on the spleen (Fig. 3). Similarly, five of six (83.3%) MCNs abutted on the spleen.

Discussion

Patients with mucinous cystic neoplasm (MCN) are exclusively female (98.1%) with a mean age of 48 years [13]. Pancreatic epidermoid cyst (EDC) is seen mostly in the fourth decade, but the male and female ratio is 1:1 [1]. All of the eight EDC cases in our series were female patients, which may reflect that the differential diagnosis of EDC vs. MCN is clinically problematic, especially when splenic tissue cannot be recognized on imaging findings. In our series, both EDC and MCN presented as a relatively thick-walled cyst with low signal intensity on T2WI and delayed enhancement, representing fibrous tissue within the cyst wall (Fig. 2). Since the signal intensity of the cyst wall of EDC was low on T2WI, it would be difficult to confirm the presence of splenic tissue within the cyst wall even with superparamagnetic iron oxide (SPIO)-enhanced MRI.

Bertolotto et al. [14] described that accessory spleen appears round with a smooth margin, while splenosis shows a lobulated margin. Similarly, an intrapancreatic accessory spleen presents as a well-circumscribed round mass [15]. Since EDC originates from an intrapancreatic accessory spleen, the shape of EDC would follow that of an accessory spleen, which may explain why EDCs tend to appear round or oval with a smooth margin.

The cyst wall (i.e., wall enhancement) could be recognized in both EDC and MCN. However, the thickness of the cyst wall was uneven and the thinnest portion was more prominent in MCN than EDC. This observation may explain why a contour deformity was seen in MCN, showing a pear-like or multilobulated shape (Figs. 4 and 5). For example, the relatively thinner portion of a cyst wall may tend to expand outward or to be compressed by surrounding structures. In addition, multiple septa may contribute to the lobulated shape of MCN.

For the differential diagnosis of EDC vs. MCN at the edge of the pancreatic tail, the first step is to look for the presence of residual splenic tissue. If residual splenic tissue is apparent, it is not necessary to evaluate the shape because EDC may not present with a round or oval shape. When residual splenic tissue cannot be appreciated, the key for the differential diagnosis between EDC and MCN would be the shape of the cystic lesions. If a cystic lesion presents with a multilobulated or pear-like margin, it is more likely MCN rather than EDC. When evaluating the shape, it is desirable to utilize multiplanar reformatted (MPR) images (Figs. 2 and 4). Since both EDC and MCN may contain high levels of proteinaceous fluid or blood products, the presence of high-intensity fluid on T1- and diffusion-weighted images may not be helpful for the differential diagnosis (Figs. 3 and 5).

There were several limitations to this study. First, this study was retrospective and there existed a selection bias. Second, the study group was small because pancreatic EDC is

uncommon and surgical resection is not usually indicated for EDC if the presence of splenic tissue is confirmed on imaging studies. Third, it has been reported that EDC is more often multilocular than unilocular [1]. Thus, endoscopic ultrasound may have more clearly demonstrated septa in EDC. Fourth, the shape patterns of cystic lesions were determined subjectively, and the observation might not be consistent in each reader. Therefore, we should have performed independent reading first, and then assessed the concordance between the two readers using kappa statistics. Finally, we have to admit that it is difficult to distinguish EDC from MCN if a cystic lesion at the edge of the pancreatic tail presents as a round or oval shape with septa (Fig. 2).

In conclusion, although imaging findings for EDC without a solid component (residual splenic tissue) and MCN overlap, a pear-like or multilobulated shape may favor the diagnosis of MCN. In patients with a round or cystic oval lesion in the pancreatic tail, epidermoid cyst should be included in the differential diagnosis.

Compliance with Ethical Standards

Conflict of Interest The authors declare that they have no conflict of interest.

References

1. Adsay NV, Hasteh F, Cheng JD, Klimstra DS. Squamous-lined cysts of the pancreas: lymphoepithelial cysts, dermoid cysts (teratomas), and accessory-splenic epidermoid cysts. Semin Diagn Pathol. 2000;17(1):56–65.
2. Yokomizo H, Hifumi M, Yamane T, Hirata T, Terakura H, Murata K, et al. Epidermoid cyst of an accessory spleen at the pancreatic tail: diagnostic value of MRI. Abdom Imaging. 2002;27(5):557–9. https://doi.org/10.1007/s00261-001-0055-2.
3. Sonomura T, Kataoka S, Chikugo T, Hirooka T, Makimoto S, Nakamoto T, et al. Epidermoid cyst originating from an intrapancreatic accessory spleen. Abdom Imaging. 2002;27(5):560–2. https://doi.org/10.1007/s00261-001-0145-1.
4. Kanazawa H, Kamiya J, Nagino M, Uesaka K, Yuasa N, Oda K, et al. Epidermoid cyst in an intrapancreatic accessory spleen: a case report. J Hepato-Biliary-Pancreat Surg. 2004;11(1):61–3. https://doi.org/10.1007/s00534-003-0844-9.
5. Itano O, Shiraga N, Kouta E, Iri H, Tanaka K, Hattori H, et al. Epidermoid cyst originating from an intrapancreatic accessory spleen. J Hepato-Biliary-Pancreat Surg. 2008;15(4):436–9. https://doi.org/10.1007/s00534-007-1243-4.
6. Motosugi U, Yamaguchi H, Ichikawa T, Sano K, Araki T, Takayama Y, et al. Epidermoid cyst in intrapancreatic accessory spleen: radiological findings including superparamagnetic iron oxide-enhanced magnetic resonance imaging. J Comput Assist Tomogr. 2010;34(2):217–22. https://doi.org/10.1097/RCT.0b013e3181c1b2bd.
7. Servais EL, Sarkaria IS, Solomon GJ, Gumpeni P, Lieberman MD. Giant epidermoid cyst within an intrapancreatic accessory spleen mimicking a cystic neoplasm of the pancreas: case report and review of the literature. Pancreas. 2008;36(1):98–100. https://doi.org/10.1097/MPA.0b013e3181359e36.
8. Gleeson FC, Kendrick ML, Chari ST, Zhang L, Levy MJ. Epidermoid accessory splenic cyst masquerading as a pancreatic mucinous cystic neoplasm. Endoscopy. 2008;40(Suppl 2):E141–2. https://doi.org/10.1055/s-2007-995735.
9. Ru K, Kalra A, Ucci A. Epidermoid cyst of intrapancreatic accessory spleen. Dig Dis Sci. 2007;52(5):1229–32. https://doi.org/10.1007/s10620-006-9376-x.
10. Kadota K, Kushida Y, Miyai Y, Katsuki N, Hayashi T, Bando K, et al. Epidermoid cyst in an intrapancreatic accessory spleen: three case reports and review of the literatures. Pathol Oncol Res. 2010;16(3):435–42. https://doi.org/10.1007/s12253-009-9229-y.
11. Jones NB, Hatzaras I, George N, Muscarella P, Ellison EC, Melvin WS, et al. Clinical factors predictive of malignant and premalignant cystic neoplasms of the pancreas: a single institution experience. HPB (Oxford). 2009;11(8):664–70. https://doi.org/10.1111/j.1477-2574.2009.00114.x.
12. Kim YS, Cho JH. Rare nonneoplastic cysts of pancreas. Clin Endosc. 2015;48(1):31–8. https://doi.org/10.5946/ce.2015.48.1.31.
13. Yamao K, Yanagisawa A, Takahashi K, Kimura W, Doi R, Fukushima N, et al. Clinicopathological features and prognosis of mucinous cystic neoplasm with ovarian-type stroma: a multi-institutional study of the Japan pancreas society. Pancreas. 2011;40(1):67–71. https://doi.org/10.1097/MPA.0b013e3181f749d3.
14. Bertolotto M, Gioulis E, Ricci C, Turoldo A, Convertino C. Ultrasound and Doppler features of accessory spleens and splenic grafts. Br J Radiol. 1998;71(846):595–600. https://doi.org/10.1259/bjr.71.846.9849381.
15. Ishigami K, Hammett B, Obuchi M, Katz D, Rayhill S, Fathala A, et al. Imaging of an accessory spleen presenting as a slow-growing mass in the transplanted pancreas. AJR Am J Roentgenol. 2004;183(2):405–7. https://doi.org/10.2214/ajr.183.2.1830405.